(Received 6 January 2025, Accepted 7 March 2025, Scheduled 17 March 2025)

Design of a High-Gain Circularly Polarized Dielectric Resonator Antenna with Dual Annular Grooves

Wenhan Wan[1,2], Wusheng Ji[1,2,*], Jinfeng Gan[1,2], Xingyong Jiang[3], and Yun Gao[1,2]

[1] *Institute of Antenna and Microwave Techniques, Tianjin University of Technology and Education, Tianjin 300222, China*
[2] *School of Electronic Engineering, Tianjin University of Technology and Education, Tianjin 300222, China*
[3] *Rofs Microsystem, Tianjin 300462, China*

ABSTRACT: This paper proposes a single-fed wideband circularly polarized high-gain dielectric resonator antenna (DRA) for millimeter waves. By cutting out a ring slot in the upper and lower parts of the cylindrical dielectric resonator antenna, higher-order modes are excited, effectively broadening the bandwidth and enhancing the gain. To achieve circular polarization, the DRA is fed by a microstrip line through an asymmetric Z-shaped slot coupling. Measurement results show that the antenna's impedance matching $S_{11} < -10$ dB bandwidth is 25.6% (35–45.31 GHz). The usable circular polarization (CP) bandwidth is found to be 8.9% (36.2–39.6 GHz), where the -10 dB input impedance bandwidth and 3-dB axial ratio bandwidth fall within the same passband, with a maximum in-band gain of 10.67 dBi. The proposed antenna employs a single-fed technique, features a simple fabrication process, exhibits excellent performance, and is suitable for FR2 band applications.

1. INTRODUCTION

With the advancement of communication technologies, the demand for accessing high-speed data and large amounts of information continues to rise alongside the increasing number of communication users, leading research and development in communication systems to focus on designs operating at millimeter-wave and even higher frequencies [1]. In the millimeter-wave and higher frequency bands, antennas exhibit significant losses, necessitating the development of high-gain antennas. Minimizing ohmic losses in antennas at millimeter-wave frequencies is a critical design metric, and researchers often employ dielectric resonator antennas to achieve this. Dielectric resonator antennas are renowned for their low ohmic losses [2, 3], ease of integration with circuits, and broadband characteristics [4–7], making them the optimal choice for designing low-loss antennas. Over the past two decades, dielectric resonator antennas have seen significant advancements and exhibit excellent properties such as compact size, light weight, wide impedance bandwidth, and high radiation efficiency [8].

In antenna applications, circularly polarized antennas are more highly regarded than linearly polarized antennas due to their advantages in reducing polarization mismatch, suppressing multipath interference [9, 10], and overcoming the effects of Faraday rotation. Circularly polarized antennas can significantly enhance the quality of wireless signal transmission. Researchers have conducted extensive studies on achieving circular polarization in antennas, and the current methods can be categorized into two types: single-feed and dual-feed techniques [11]. Compared to single-feed techniques, dual-feed techniques can more easily achieve a wider 3 dB axial ratio bandwidth, but they introduce new issues, such as complex power division networks and hybrid coupling networks, leading to complicated antenna structure designs and increased overall size.

Various approaches exist for realizing circular polarization with single-feed techniques, including custom dielectric resonator geometries, specialized feeding slot configurations, layered dielectric resonator designs, and the incorporation of metasurfaces and air vias. In [12], a stepped-shape dielectric resonator antenna (DRA) was employed, fed by a microstrip line and excited through a hybrid split-ring and full-ring grounding scheme, resulting in an 8.47% 3 dB axial ratio bandwidth and a gain of 7.6 dBi. In [13], a feeding structure incorporating a bent microstrip line was introduced to produce circular polarization, attaining a 12.26% axial ratio bandwidth and a gain of 2.35 dBi. In [14], an S-shaped stacked DRA was utilized, significantly improving the axial ratio bandwidth to 24.75% and achieving a gain of 7.32 dBi. In [15], a self-complementary metasurface-based approach was proposed, enabling circular polarization and a gain of 6.03 dBi by leveraging the quasi-self-complementary properties of the metasurface. In [16], annular air vias were implemented, resulting in a 5.5% axial ratio bandwidth and a gain of 7.1 dBi. In [17], dielectric via technology was employed to increase bandwidth by treating the perforated substrate as a DRA, achieving a 26.7% axial ratio bandwidth. The aforementioned references have made significant improvements and breakthroughs in antenna circular polarization, but these studies have not sufficiently addressed gain performance; although circular polarization was achieved, it also resulted in reduced gain, limiting the application of DRAs.

To address the issue of low gain in existing single-fed circularly polarized antennas, this paper proposes a simple single-feed technique that achieves wideband circular polarization and

* Corresponding author: Wusheng Ji (jiwusheng@tute.edu.cn).

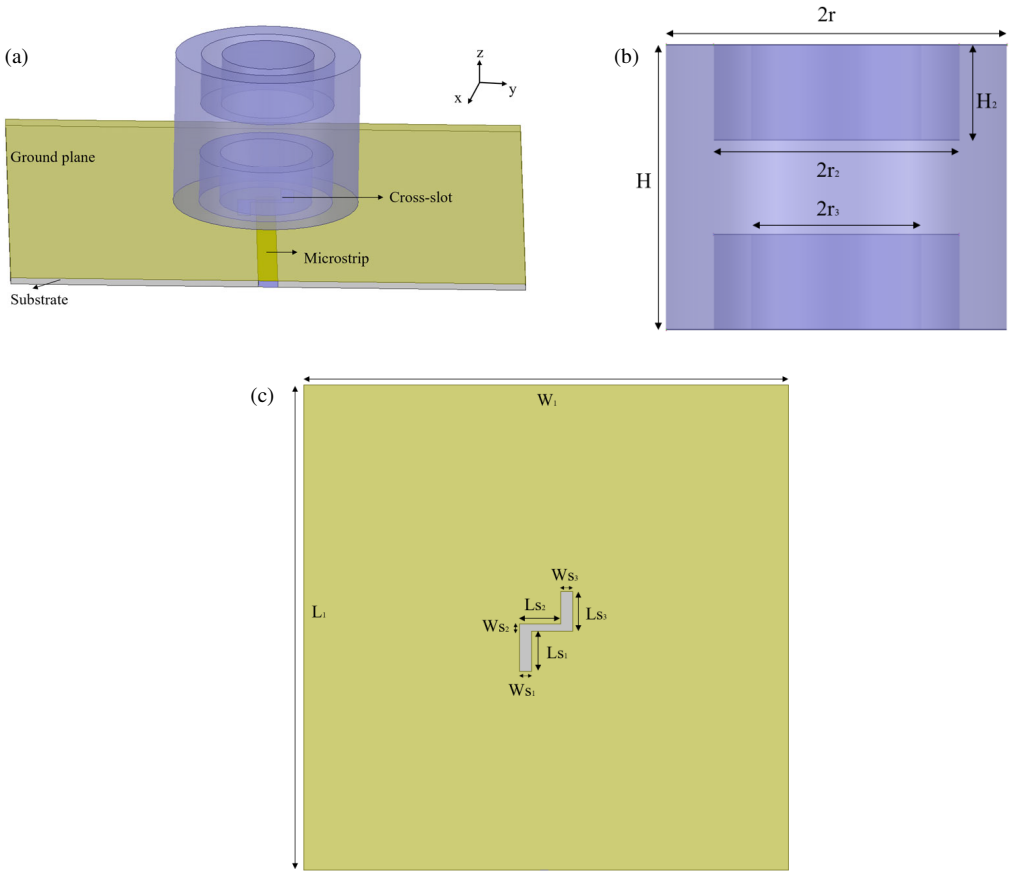

FIGURE 1. Configuration of the proposed antenna. (a) 3D view. (b) Bottom view. (c) Top view of Z-shaped groove.

high gain by using an asymmetric Z-shaped slot feed combined with a cylindrical dielectric resonator with a cut ring slot. Both simulation and measurement results validate the excellent performance of the proposed antenna.

2. ANTENNA DESIGN AND ANALYSIS

2.1. Antenna Structure

The proposed dielectric resonator antenna (DRA) in this paper, as shown in Figure 1, consists of a cylindrical dielectric resonator at the top and a feeding substrate at the bottom. The cylindrical DRA structure at the top is made of JJD07-1 dielectric ceramic material (with a relative permittivity $\varepsilon_r = 6.7$), with a height of H and a radius of r. A ring slot is cut out in the upper and lower parts of the cylindrical DRA, with a slot width of r_1, an outer ring radius of r_2, an inner ring radius of r_3, and a height of H_2 The bottom feeding substrate is made of a Rogers 5880 dielectric substrate, with a relative permittivity of 2.2, a loss tangent of 0.0009, and a thickness of h. The upper surface of the dielectric substrate serves as the ground plane, with a Z-shaped slot etched along the X-axis at the center of the ground plane, having geometric parameters Ls_1, Ls_2, Ls_3, Ws_1, Ws_2, and Ws_3. The feeding microstrip line is attached to the bottom surface of the dielectric substrate, symmetrically placed along the X-axis. The specific dimensions of the antenna are listed in Table 1.

TABLE 1. Antenna geometry.

Parameters	H	r	r_1	r_2	r_3	H_2	h
Value/mm	6	8	0.8	2.6	1.8	2	0.254
Parameters	Ls_1	Ls_2	Ls_3	Ws_1	Ws_2	Ws_3	
Value/mm	1.8	1.7	1.6	0.5	0.35	0.5	

2.2. Antenna Design Process

As shown in Figure 2, the design process of the proposed antenna is clearly illustrated. Figure 2(a) shows Antenna 1, which features a classic cylindrical dielectric resonator at the top. Figure 2(b) depicts Antenna 2, which adds a ring slot to the lower part of Antenna 1. Figure 2(c) presents the proposed antenna in this paper, which adds a ring slot to the upper part of Antenna 2, with the upper and lower ring slots having identical geometric dimensions and being symmetrically placed. The introduction of the ring slots is equivalent to incorporating air media into the dielectric resonator (DRA) structure, reducing the resonator's dielectric constant, enhancing the antenna's radiation capability, and broadening its operating bandwidth. Additionally, the upper and lower ring slot structures excite higher-order modes in the dielectric resonator antenna, increasing its gain; the higher-order modes introduce slight perturbations in the electric field, enhancing the antenna's circular polarization performance.

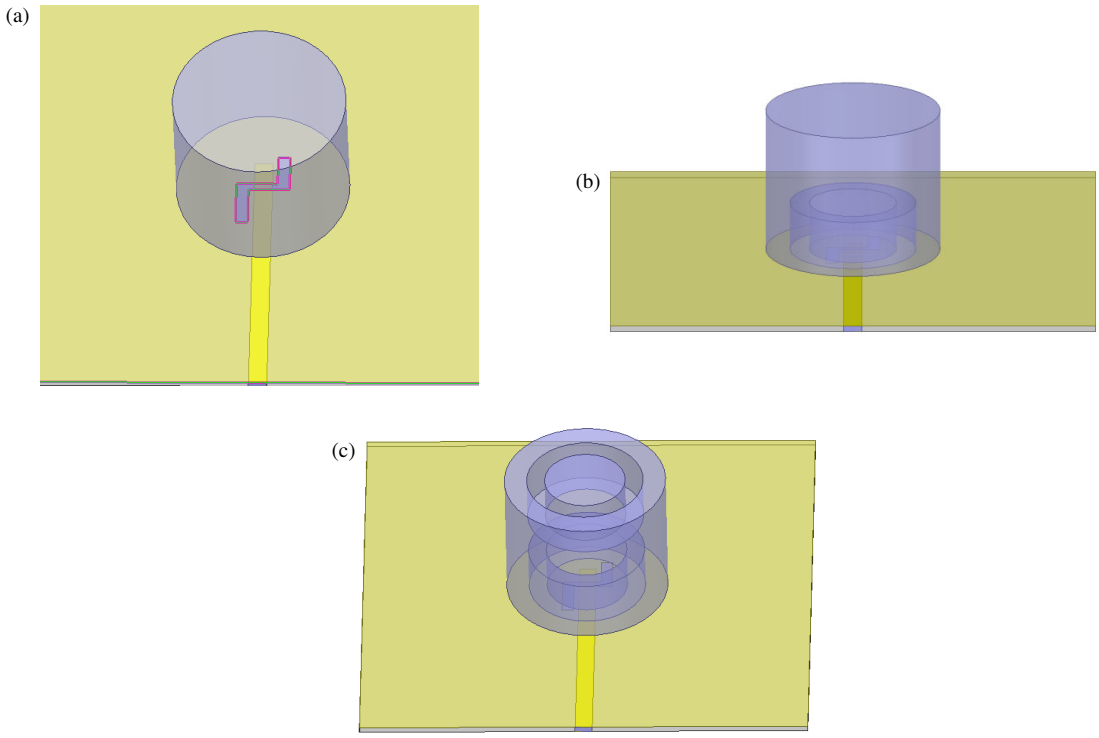

FIGURE 2. The proposed antenna and two reference antennas. (a) Antenna 1. (b) Antenna 2. (c) The proposed antenna.

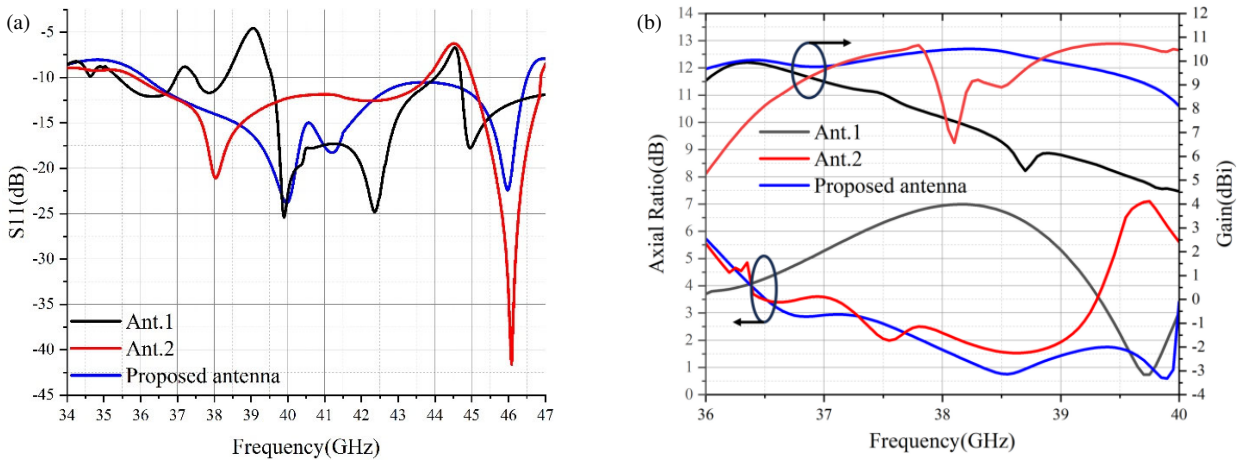

FIGURE 3. Reflection coefficient axial ratio and gain of the proposed antenna compared with two reference antennas. (a) Reflection coefficient curves. (b) Axial ratio and gain curves.

A comparison of the performance of the proposed antenna with Antenna 1 and Antenna 2 is shown in Figure 3, demonstrating that the introduction of the ring slots significantly broadens the antenna's operating bandwidth, axial ratio bandwidth, and improves the gain, with the gain curve being relatively stable.

2.3. Working Principle of the Proposed Antenna

The resonant frequency of the DRA can be preliminarily determined using the Dielectric Waveguide Model (DWM). It is assumed that the surface of the DRA is an ideal magnetic conductor. Under these conditions, the wave functions for the Transverse Electric (TE) and Transverse Magnetic (TM) modes of the DRA can be expressed as follows:

$$\psi_{TE_{npm}} = J_n\left(\frac{2X_{np}}{D}\rho\right)\begin{pmatrix}\sin(n\phi)\\ \cos(n\phi)\end{pmatrix}\sin\left[\frac{(2m+1)\pi z}{2H}\right] \quad (1)$$

$$\psi_{TM_{npm}} = J_n'\left(\frac{2X_{np}'}{D}\rho\right)\begin{pmatrix}\sin(n\phi)\\ \cos(n\phi)\end{pmatrix}\cos\left[\frac{(2m+1)\pi z}{2H}\right] \quad (2)$$

where J_n is the Bessel function of the first kind, with $J_n(X_{np}) = 0$ and $J_n'(X_{np}') = 0, n = 1, 2, 3, ..., p = 1, 2, 3, ..., m = 1, 2, 3, ...$

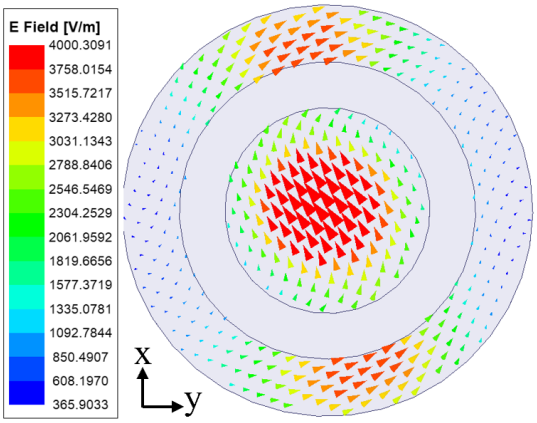

FIGURE 4. Electric field at 40 GHz.

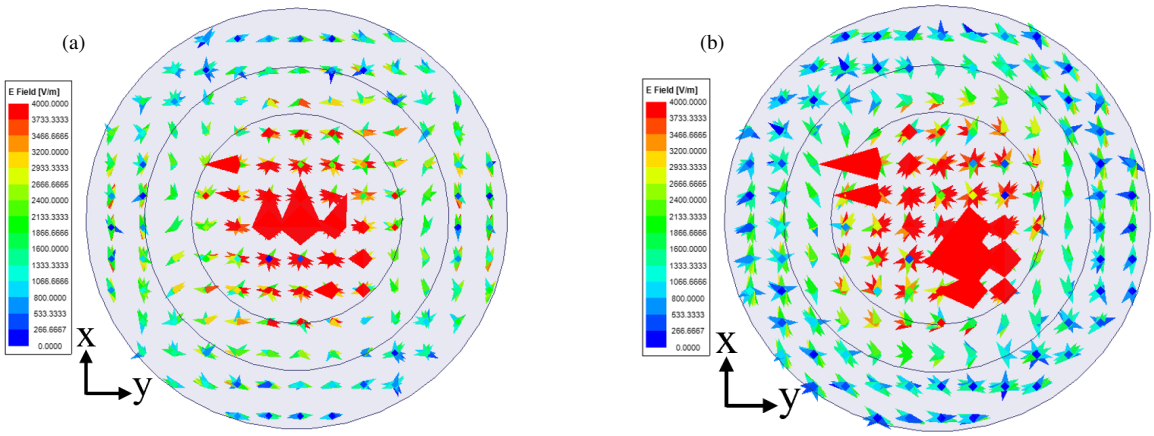

FIGURE 5. Electric field at 38.5 GHz. (a) $\phi = 0°$. (b) $\phi = 90°$.

From the separation equation $k_\rho^2 + k_z^2 = k^2 = \omega^2\mu\varepsilon$, the resonant frequency of the cylindrical DRA for npm mode can be calculated by the following formula:

$$f_{npm} = \frac{1}{\pi D\sqrt{\mu\varepsilon}}\sqrt{\left(\begin{array}{c} X_{np}^2 \\ X_{np}'^2 \end{array}\right) + \left[\frac{\pi D}{4H}(2m+1)\right]^2} \quad (3)$$

where $\varepsilon = \varepsilon_0 \times \varepsilon_r$.

To investigate the working principle of the proposed antenna, the electric field distribution of the antenna was simulated. Figure 4 shows the electric field distribution of the antenna at 40 GHz. From Figure 4, it can be observed that at 40 GHz, the field strength in the outer ring DRA region is also high, confirming that the DRA excites the $HEM_{12\delta}$ mode, which alters the electric field distribution of the dominant mode. Due to the highly symmetric field distribution of the $HEM_{12\delta}$ mode, the radiated energy is concentrated in the main radiation direction, thereby improving the antenna's directivity and gain.

To further analyze the mechanism of the antenna radiating circularly polarized waves, Figure 5 presents the electric field vector diagrams of the DRA at $\phi = 0°$ and $\phi = 90°$ at the axial ratio minimum point of 38.5 GHz. Since the electric field distribution in Figure 5(a) has a weak component in the x-direction, but it has one peak and two nodes in all three directions, the mode is quasi-TE_{111}^x. Similarly, the modes in Figure 5(b) are identified as quasi-TE_{111}^y. From 0° to 90°, the electric field vector rotates 90 degrees counterclockwise around the $+Z$ axis, and the magnitudes are approximately equal, enabling this pair of orthogonal modes to radiate a relatively standard right-hand circularly polarized wave.

2.4. Parametric Analysis

To describe the influence of air on the performance of the dielectric resonator, a parametric analysis of the width (r_1) and height (H_2) of the circular slot was conducted, as shown in Figure 6. In Figure 6(a), as r_1 increases, the S-parameter curve tends to shift toward higher frequencies; however, if the width is too large, it causes impedance mismatch, preventing proper radiation, so the width of the circular slot can only be adjusted within a small range. The reason is that if the air gap is too large, the electric field excited by the microstrip-Z-slot coupling feed cannot effectively induce resonance in the dielectric resonator. When $r_1 = 0.8$ mm, the antenna achieves good impedance matching. As can also be seen in Figure 6(a), the gain gradually increases with the increase of r_1. Therefore, considering all factors, r_1 is chosen to be 0.8 mm. H_2 is the height of the circular slot. In Figure 6(c), when $H_2 = 2$ mm, the antenna achieves the best impedance matching. As shown

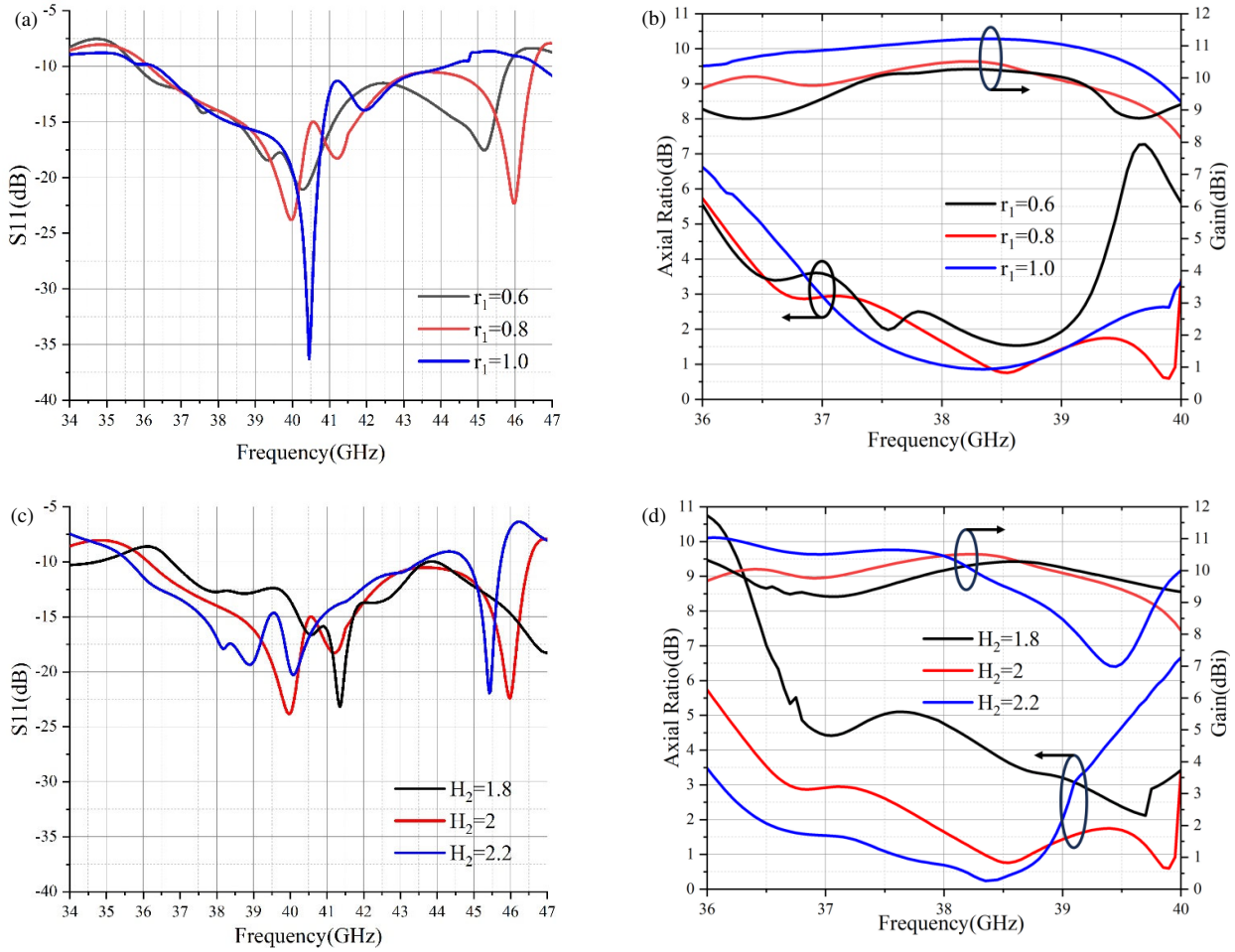

FIGURE 6. Parametric study of reflection coefficient, gain and axial ratio. (a) Antenna reflection coefficient variation with r_1. (b) Antenna axial ratio and gain variation with r_1. (c) Antenna reflection coefficient variation with H_2. (d) Antenna axial ratio and gain variation with H_2.

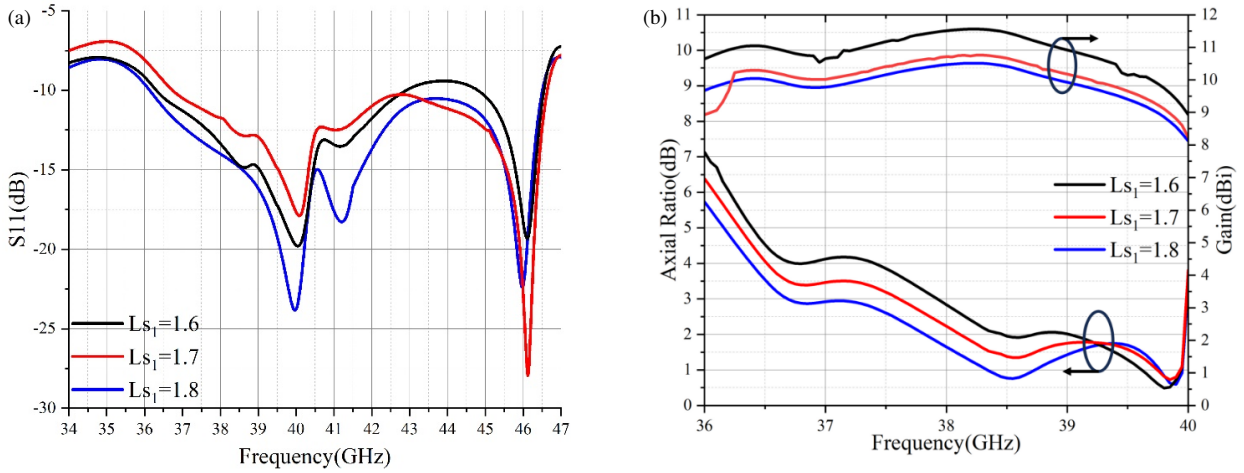

FIGURE 7. Parametric study of reflection coefficient, gain and axial ratio. (a) Antenna reflection coefficient variation with Ls_1. (b) Antenna axial ratio and gain variation with Ls_1.

in Figure 6(d), both the antenna's gain and axial ratio bandwidth increase with H_2, but when $H_2 = 2.2$ mm, a sharp drop occurs at higher frequencies. Therefore, after comprehensive consideration, H_2 is chosen to be 2.0 mm.

To analyze the influence of the Z-shaped slot on the performance of the dielectric resonator, its key parameters were scanned, and the results are shown in Figure 7. Ls_1 is the length of the long side of the Z-shaped slot. In Figure 7(a), when $Ls_1 = 1.6$ mm, some frequency points exceed -10 dB; when

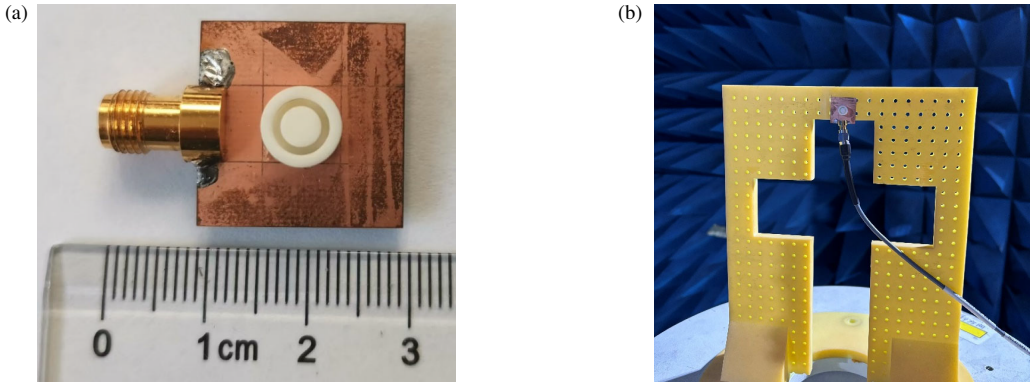

FIGURE 8. Antenna prototype. (a) Photograph of the antenna prototype. (b) Photograph of microwave anechoic chamber measurement.

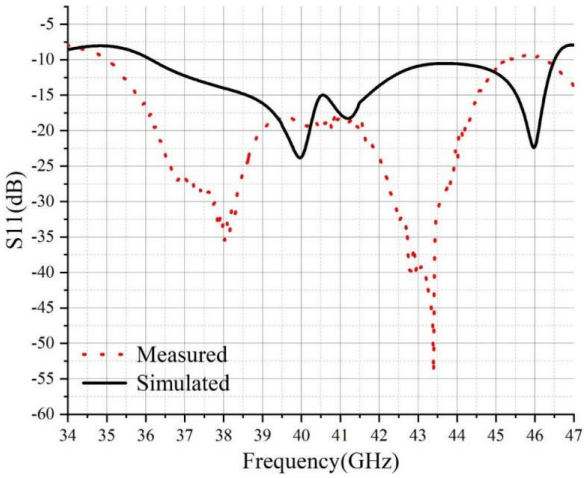

FIGURE 9. Measured and simulated reflection coefficients of the proposed antenna.

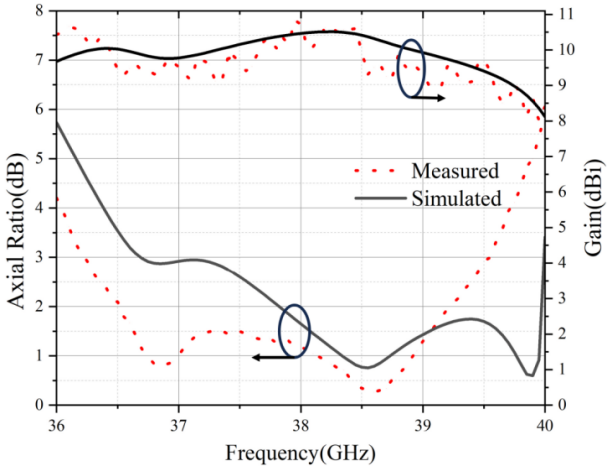

FIGURE 10. Measured and simulated axial ratios and gains of the proposed antenna.

$Ls_1 = 1.8$ mm, the impedance bandwidth is 25.1%; as Ls_1 gradually increases, the impedance bandwidth also increases; at $Ls_1 = 1.8$ mm, the antenna achieves good impedance matching. In Figure 7(b), as Ls_1 gradually increases, the axial ratio bandwidth increases, while the gain gradually decreases. Since the gains at $Ls_1 = 1.7$ mm and $Ls_1 = 1.8$ mm are very close, considering both the impedance bandwidth and axial ratio bandwidth, $Ls_1 = 1.8$ mm is selected.

3. RESULT AND DISCUSSION

The cylindrical dielectric resonator was fabricated using mechanical machining, and the feeding substrate was produced using PCB technology. After assembly, measurements were conducted in an anechoic chamber to verify the antenna's performance. The antenna prototype is shown in Figure 8(a). Figure 8(b) shows the scenario of the antenna prototype being measured for gain in the anechoic chamber.

Figure 9 shows the simulated and measured impedance bandwidth curves of the antenna. The simulated and measured DRAs have -10 dB input impedance bandwidths of 25.1% (36.14–46.52 GHz) and 25.6% (35–45.31 GHz), respectively. Since the DRA is fabricated using mechanical machining, there are manufacturing errors; additionally, the air gap between the bottom feeding substrate and top DRA during antenna assembly also introduces errors. These two factors result in certain discrepancies between the simulation and measurement curves.

Figure 10 shows the simulated and measured axial ratio and gain curves of the proposed antenna. As can be seen from Figure 10, the simulated and measured axial ratio bandwidths of the antenna reach 8.6% (36.65–39.95 GHz) and 8.9% (36.2–39.6 GHz), respectively. The axial ratio bandwidths are usable because they all fall within the impedance bandwidth. Moreover, within the axial ratio bandwidth, a flat high gain is observed, with the measured maximum gain reaching 10.67 dBi.

Figure 11 shows the radiation pattern of the fabricated DRA at the frequency of minimum axial ratio, which is 38.5 GHz. As expected, broadside patterns are obtained in both the $\phi = 0°$ and $\phi = 90°$ planes. For these two planes, the field in the right-hand circular polarization (RHCP) direction is more than 29.8 dBi stronger than that in the left-hand circular polarization (LHCP) direction, confirming that it is a good RHCP antenna.

Table 2 presents a comparison between the proposed antenna in this paper and existing millimeter-wave circularly polarized DRAs in the literature. Compared to [15], the proposed antenna demonstrates significant advantages in terms of bandwidth and

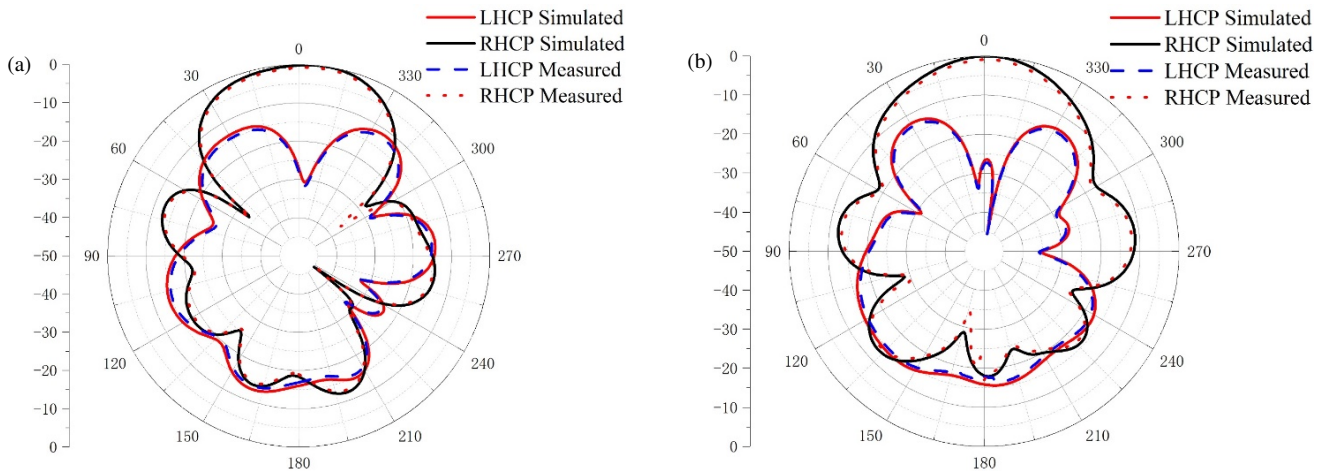

FIGURE 11. Radiation patterns of proposed antenna at 38.5 GHz. (a) $\phi = 0°$. (b) $\phi = 90°$.

TABLE 2. Comparison with previously reported work in literature.

Ref.	Impedance BW (sim./exp.) (%)	Overlapping BW (sim./exp.) (%)	Gain max (sim./exp.) (%)	Structure
[15]	-/0.05	-/0.01	6.67/6.03	Simple
[18]	15.5/11.88	3.3/9.8	10.35/10.3	Simple
[19]	8.23/8.26	2.79/2.97	15.6/15.5	Simple
[20]	45/35	22.6/19.3	-/10	Complicated
Proposed work	25.1/25.6	8.6/8.9	10.52/10.67	Simple

gain. Compared to [18], although the gains of the two antennas are similar, the proposed antenna has higher impedance bandwidth and axial ratio bandwidth. Compared to [19], the proposed antenna has a lower gain but significantly higher impedance bandwidth and axial ratio bandwidth. Compared to [20], the gains of the two antennas are similar, but the proposed antenna has lower impedance bandwidth and axial ratio bandwidth. However, the antenna in [20] has a complex structure, making it difficult to fabricate. In summary, the proposed antenna demonstrates high application value in the millimeter-wave frequency band.

4. CONCLUSION

This paper designs a method for achieving a wideband circularly polarized antenna by exciting a dielectric resonator using a Z-shaped slot. By using a Z-shaped slot feed to generate orthogonal modes, higher-order modes of the dielectric resonator are excited, effectively enhancing the antenna's gain and bandwidth. The introduction of air media into the cylindrical dielectric resonator reduces the resonator's dielectric constant and enhances the antenna's radiation capability. The proposed antenna offers advantages such as wide bandwidth, circular polarization, and high gain, along with a simple structure, straightforward feeding mechanism, and low cost. It operates in the millimeter-wave frequency band and has promising applications in 5G communication systems.

ACKNOWLEDGEMENT

This work is supported by Tianjin Key Projects of Research and Development and Science and Technology Support in 2020 (20YFZCGX00700), and Tianjin Enterprise Science and Technology Commissioner Project in 2022 (22YDTPJC00330).

REFERENCES

[1] Rappaport, T. S., Y. Xing, G. R. MacCartney, A. F. Molisch, E. Mellios, and J. Zhang, "Overview of millimeter wave communications for fifth-generation (5G) wireless networks — With a focus on propagation models," *IEEE Transactions on Antennas and Propagation*, Vol. 65, No. 12, 6213–6230, Aug. 2017.

[2] Mongia, R. K. and P. Bhartia, "Dielectric resonator antennas — A review and general design relations for resonant frequency and bandwidth," *International Journal of Microwave and Millimeter-Wave Computer-Aided Engineering*, Vol. 4, No. 3, 230–247, Jul. 1994.

[3] Leung, K. W., E. H. Lim, and X. S. Fang, "Dielectric resonator antennas: From the basic to the aesthetic," *Proceedings of the IEEE*, Vol. 100, No. 7, 2181–2193, Apr. 2012.

[4] Simeoni, M., R. Cicchetti, A. Yarovoy, and D. Caratelli, "Plastic-based supershaped dielectric resonator antennas for wide-band applications," *IEEE Transactions on Antennas and Propagation*, Vol. 59, No. 12, 4820–4825, Aug. 2011.

[5] Keyrouz, S. and D. Caratelli, "Dielectric resonator antennas: Basic concepts, design guidelines, and recent developments at millimeter-wave frequencies," *International Journal of Antennas and Propagation*, Vol. 2016, No. 1, 6075680, 2016.

[6] Cicchetti, R., E. Miozzi, and O. Testa, "A novel wideband multi-permittivity composite dielectric resonator antenna for wireless applications," in *2016 IEEE-APS Topical Conference on Antennas and Propagation in Wireless Communications (APWC)*, 70–73, Cairns, QLD, Australia, Sep. 2016.

[7] Cicchetti, R., E. Miozzi, and O. Testa, "Wideband and uwb antennas for wireless applications: A comprehensive review," *International Journal of Antennas and Propagation*, Vol. 2017, No. 1, 2390808, 2017.

[8] Yang, M., Y. Pan, and W. Yang, "A singly fed wideband circularly polarized dielectric resonator antenna," *IEEE Antennas and Wireless Propagation Letters*, Vol. 17, No. 8, 1515–1518, Jun. 2018.

[9] Mongia, R. K. and P. Bhartia, "Dielectric resonator antennas — A review and general design relations for resonant frequency and bandwidth," *International Journal of Microwave and Millimeter-Wave Computer-Aided Engineering*, Vol. 4, No. 3, 230–247, Jul. 1994.

[10] Toh, B. Y., R. Cahill, and V. F. Fusco, "Understanding and measuring circular polarization," *IEEE Transactions on Education*, Vol. 46, No. 3, 313–318, Aug. 2003.

[11] Petosa, A., *Dielectric Resonator Antenna Handbook*, 308, Artech House, 2007.

[12] Dash, U. A., D. Dutta, and S. Pahadsingh, "Circularly polarized stepped rectangular DRA for mid-band 5G application," in *2023 IEEE 3rd International Conference on Applied Electromagnetics, Signal Processing, & Communication (AESPC)*, 1–4, Bhubaneswar, India, Nov. 2023.

[13] Kumar, R., D. K. Choudhary, R. Singh, and R. K. Chaudhary, "A wideband circularly polarized DRA excited with meandered-line inductor for Wi-MAX/LTE2500 applications," in *2017 Progress In Electromagnetics Research Symposium — Fall (PIERS — FALL)*, 1514–1519, Singapore, Nov. 2017.

[14] Varshney, G., "Gain and bandwidth enhancement of a singly-fed circularly polarised dielectric resonator antenna," *IET Microwaves, Antennas & Propagation*, Vol. 14, No. 12, 1323–1330, Oct. 2020.

[15] Zhao, G., Y. Zhou, J. R. Wang, and M. S. Tong, "A circularly polarized dielectric resonator antenna based on quasi-self-complementary metasurface," *IEEE Transactions on Antennas and Propagation*, Vol. 70, No. 8, 7147–7151, Jan. 2022.

[16] Elahi, M., A. Altaf, Y. Yang, K.-Y. Lee, and K. C. Hwang, "Circularly polarized dielectric resonator antenna with two annular vias," *IEEE Access*, Vol. 9, 41 123–41 128, Mar. 2021.

[17] Tong, C., H. I. Kremer, N. Yang, and K. W. Leung, "Compact wideband circularly polarized dielectric resonator antenna with dielectric vias," *IEEE Antennas and Wireless Propagation Letters*, Vol. 21, No. 6, 1100–1104, Mar. 2022.

[18] Perron, A., T. A. Denidni, and A. R. Sebak, "Circularly polarized microstrip/elliptical dielectric ring resonator antenna for millimeter-wave applications," *IEEE Antennas and Wireless Propagation Letters*, Vol. 9, 783–786, Aug. 2010.

[19] Akbari, M., S. Gupta, M. Farahani, A. R. Sebak, and T. A. Denidni, "Gain enhancement of circularly polarized dielectric resonator antenna based on FSS superstrate for MMW applications," *IEEE Transactions on Antennas and Propagation*, Vol. 64, No. 12, 5542–5546, Nov. 2016.

[20] Attia, H., A. Abdalrazik, M. S. Sharawi, and A. A. Kishk, "Wideband circularly polarized millimeter-wave DRA array for internet of things," *IEEE Internet of Things Journal*, Vol. 10, No. 11, 9597–9606, Jan. 2023.